

# Zonal Mean Circulation at the Cloud Level on Venus: Spring and Fall 1979 OCPP Observations

SANJAY S. LIMAYE

*Space Science and Engineering Center, University of Wisconsin–Madison, 1225 West Dayton Street,  
Madison, Wisconsin 53706*

AND

CHRISTIAN J. GRUND<sup>1</sup> AND STEVEN P. BURRE<sup>2</sup>

*Sigma Data Service Corporation, Institute for Space Studies, 2880 Broadway, New York, New York 10025*

Received January 28, 1982; revised May 14, 1982

Cloud motions were obtained from a number of images acquired in reflected solar ultraviolet light during spring and fall of 1979 from the Pioneer Venus Orbiter Cloud Photopolarimeter (OCPP) to determine the zonal mean circulation of the atmosphere of Venus at the cloud top level. The meridional profile of the zonal component of motion is somewhat different from that previously obtained from Mariner 10 and preliminary Pioneer Venus observations, although the equatorial magnitude is about the same ( $-94$  m/sec). The mean meridional motion is toward the south pole south of about  $5^\circ$  south latitude, and toward the north pole north of this latitude, with peak mean magnitudes of about  $7$  m/sec polewards of  $20^\circ$  north and  $40^\circ$  south latitudes in the respective hemispheres. From the few measurements obtained at higher latitudes the magnitude of the mean meridional component appears to decrease although it is still directed toward the respective poles. Due to the evolution of the cloud patterns over the duration of the images from which the cloud velocities are obtained, the uncertainties in the mean zonal and meridional components may be as large as  $5$ – $10$  and  $2$ – $4$  m/sec, respectively. Preliminary estimates of meridional momentum transport show that the mean circulation dominates the eddy circulation transport completely, in agreement with the estimates obtained from Mariner 10 data, although the uncertainties in both the mean and eddy circulation transports are large. The momentum transports are polewards and their peak magnitudes occur at latitudes between  $20^\circ$  and  $40^\circ$  in both the hemispheres.

## 1. INTRODUCTION

Continued observations of the Venus atmospheric circulation at the cloud top level indicate that the circulation is quite variable although it retains its basic characteristics: largely zonal and retrograde motions with equatorial speed of about  $95$  m/sec. Preliminary results on the atmospheric circulation

at the cloud top level obtained from the Pioneer Venus data as reported by Rossow *et al.* (1980) show that the meridional profile of the mean zonal component of motion was quite different from that observed during the Mariner 10 encounter (Suomi, 1974; Limaye, 1977; Travis, 1978; Schubert *et al.*, 1980; Limaye and Suomi, 1981). The most prominent feature of the Pioneer observations is the absence of the strong midlatitude jet. In this paper we present independent observations of the zonal mean circulation deduced from the Pioneer Venus Orbiter images that substantiate the somewhat different circulation in the Venus atmosphere at the time of Pioneer observa-

<sup>1</sup> Current address: Department of Meteorology, University of Wisconsin–Madison, 1225 West Dayton Street, Madison, Wisconsin 53706.

<sup>2</sup> Current address: Department of Computer Science, University of Oklahoma, Norman, Oklahoma 73069.

tions. It is assumed that the somewhat longer time interval between the Pioneer images does not make cloud motion estimates unreliable at some latitudes although no direct evidence of such problems is available. The results presented here were obtained from some of the same images analyzed by Rossow *et al.* (1980), although the method used is different. Rossow *et al.* presented results obtained by digital correlation of  $32 \times 32$  image elements (equivalent to approximately  $800 \times 800$ -km-sized features), whereas the present results were obtained by visually identifying cloud features and tracking them in paired images. The time period covered in the present analysis is also somewhat longer, although the total number of cloud motion vectors obtained is considerably less due to the nature of tracking. Although the results on the mean circulation of the Venus atmosphere at the cloud top level presented here are in general agreement with those presented by Rossow *et al.* (1980) from digital tracking, some systematic differences exist that cannot be attributed to measurement errors or, the different sample of cloud vectors obtained in each case, but, rather, they reflect the differences in the techniques.

Pioneer Venus images present some special problems in the task of determining cloud motion vectors as a means of studying the true atmospheric circulation. Due to the spin-scan imaging technique used by the OCPP, the amount of time required to acquire one complete full-disk image of Venus is approximately 4 hr, compared to the instantaneous "snapshots" obtained by the Mariner 10 television cameras. The resulting poor temporal resolution makes cloud tracking somewhat difficult due to the changes in the cloud patterns over the intervening time. Since cloud tracking is the only viable means of obtaining crucial information about the mean atmospheric circulation on Venus, we are forced to test various methods of obtaining the cloud motion information in an efficient but reliable manner. One technique is the one used by Ros-

sow *et al.*, in which the digital cloud brightness pattern in one image is correlated with the pattern around a predicted location in another image acquired immediately after the first one. The relative displacement at which the correlation is maximum is then taken as the best estimate of the cloud movement. Due to the evolution of the cloud features during the two images the coefficient of correlation becomes more and more unreliable as the cloud size selected for correlation becomes smaller and smaller. The  $32 \times 32$ -element image portion used in the results reported by Rossow *et al.* (1980) was a compromise between using a small enough cloud size to ensure that the resultant velocity information is close to the true atmospheric motion and yet large enough to obtain a reliable estimate of the displacement in terms of the correlation coefficient.

The same considerations also apply to the second technique for cloud tracking, the so-called manual tracking in which the clouds are selected and tracked visually. In this case, however, the operator making the measurements is guided by the general behavior of the cloud features and their movements, and undoubtedly, experience. The danger with this technique, however, is that a particular operator may be highly selective in tracking target clouds and thus may come up with a biased estimate of the cloud motions.

In view of the drawbacks facing both the digital and the manual tracking techniques, it was thought highly desirable to use both the techniques to estimate the zonal mean circulation from the OCPP data. In order to discover whether a significant amount of bias was present in manual tracking, two independent sets of measurements were obtained on the same basic set of images. The differences between the two independent manual estimates of the mean circulation are then a reasonable estimate of the uncertainty in the mean circulation as determined by the manual technique, and the differences between other techniques such as the

digital technique may also reflect the uncertainties in our knowledge of the mean circulation on Venus. In this paper we present a comparison of two manual estimates of the cloud top level mean circulation only.

While the images in which ultraviolet clouds were tracked were obtained over some 29 orbits, they were spread in time over more than 8 months (24 days during terrestrial spring and 5 days during terrestrial fall of 1979). The spring imaging period spanned over 50 days. Thus, while detailed daily variations in the cloud top circulation cannot be ascertained due to relatively large errors in the daily mean circulation, it is possible to look for a change in the mean circulation over the intervening period of about 8 months between spring and fall 1979 in Orbiter Cloud Photopolarimeter (OCP) observations. These changes are small and comparable to the errors involved, but consistent at many latitudes. We obtained two independent measurements of cloud motions from the same set of images with a view toward isolating any bias in sampling and measurement. The results on the mean circulation obtained from each set were found to be in excellent agreement as presented below.

## 2. NATURE OF THE DATA

The basic data used in this work are the images acquired by the OCP instrument. A description of this instrument is given by Russell *et al.* (1977) and by Travis (1979). The results obtained from the OCP experiment are presented by Travis *et al.* (1979a,b), Kawabata *et al.* (1980), Rossow *et al.* (1980), and by Del Genio and Rossow (1982) in this issue. Very briefly, the OCP images are obtained by spin-scan technique from a telescope with an ultraviolet (uv) detector at the focus. Translation of the scans on Venus is provided by the motion of the spinning spacecraft in its 0.84 eccentricity orbit around Venus. The telescope is not moved during the course of a single full-disk image. For the purpose of cloud tracking, this raw image data is not suitable be-

cause of the constantly changing perspective that makes cloud tracking difficult. This raw data is navigated, i.e., located in terms of Venus coordinates, using the imaging geometry and a knowledge of the spacecraft orbit and reformatted into a standard latitude-longitude map with  $0.25^\circ$  resolution in both latitude and longitude directions.

All usable full-disk images obtained during the 1979 spring and fall observing periods were navigated and mapped in this manner, and were used for tracking clouds. The number of vectors obtained on each day of OCP imaging observations for the two sets of measurements are given in Table I. The phase angle of all the images measured is between  $20^\circ$  and  $60^\circ$ , and both the spring and fall images favor the after-

TABLE I  
NUMBER OF CLOUD MOTION VECTORS

Year	Day	Set A	Set B
79	39	401	257
79	40	219	125
79	41	313	195
79	42	116	223
79	43	114	66
79	44	126	102
79	46	120	120
79	47	394	144
79	48	234	205
79	49	206	228
79	50	297	184
79	51	202	127
79	60	118	106
79	61	71	60
79	62	141	122
79	63	129	119
79	64	0	86
79	66	0	128
79	67	125	123
79	71	138	119
79	83	69	60
79	85	78	73
79	88	60	53
79	285	126	123
79	286	111	105
79	287	0	93
79	288	0	121
79	289	0	130

noon hemisphere to varying degrees. Due to the fact that the periapsis occurs at about  $20^\circ$  north latitude, the OCPP images do not show the very high latitudes in the northern hemisphere, and thus the sampling is somewhat biased toward the southern latitudes.

### 3. TRACKING PROCEDURE

The processed images were displayed on a quasi-interactive image display device. Although the images are made up of 8-bit digital data (256 gray levels maximum), hardware limitations allowed only 16 gray levels of each image to be displayed and a maximum of only three images could be loaded onto three separate frames for rapid flipping from one frame to another. Computer software enhancements during the course of the analysis increased the number of distinct displayable gray levels of each image to 46 and was extremely beneficial to cloud tracking. The displayed image could be enhanced by choosing different colors based on the actual image brightness values. Thus in the early stages, although only 16 gray levels could be displayed, through proper use of colors and enhancements of the displayed data it was possible to identify even the low-contrast features seen in the ultraviolet images of Venus. The second set of measurements (set B) was obtained with the 46-gray level display exclusively.

During the two 1979 observing periods, typically only two or three full-disk images were obtained per each 24-hr orbit of the spacecraft, spaced approximately 4.5 hr apart. Thus some cloud features could be seen in all three images acquired on a given orbit. Whenever possible all three images were used for tracking and were displayed in a 3-frame loop. An operator then moved a cursor with the help of a trackball to locate a particular cloud visible in consecutive images, thus enabling the host computer to record the map coordinates of the cloud. Wind velocities, as well as the zonal

and meridional components of motion relative to the Venus coordinates, were calculated subsequently using these coordinates. The zonal component of motion is obtained by dividing the longitudinal displacement of the candidate cloud in meters by the elapsed time in seconds, while the meridional component is obtained similarly from the meridional displacement of the cloud, to yield wind components in metric units. The resultant cloud motion vector is assigned a latitude and longitude corresponding to the average of the initial and final positions of the cloud. The elapsed time is calculated for the actual spacecraft observation times of the cloud rather than approximating it by the difference of the image center times. The tracking procedure is thus similar to the one described by Limaye and Suomi (1981), and comments made therein about manual tracking apply in the present case also.

Initially two individuals made cloud coordinate measurements in the available images. Subsequently another individual measured cloud locations in the same set of images independently, thus yielding a different sample of vectors. This duplication of effort allowed comparisons to be made between the two sets (hereafter called sets A and B, respectively). No effort was made to track the same cloud features in the second set, and the measurements were made without the benefit of knowledge of the results from the first set. The only expectation was that the total number of measurements in each of the two sets be roughly equal, so that they could be compared to each other in an easy manner. The object was mainly to see if the results showed any operator bias in tracking. Images on 5 days were not available while set A was being generated, and are missing therein, but those images were included for set B. Although set B contains about 300 fewer vectors, a greater fraction were obtained on image pairs rather than over image triplets (1125 for set A vs 470 for set B). The results of the comparisons are presented below.

#### 4. SOURCES OF ERROR IN THE MEAN CIRCULATION

The basic aim of the study is to obtain the zonally averaged estimates of the zonal and the meridional components of motion, as well as estimates of meridional momentum transports. These quantities are obtained by averaging individual measurements as described below. The term "zonal averaging" is used liberally here in the sense that although the cloud motions are available over only a part of the dayside and none of the nightside of Venus, the resultant "average," when taken over a period longer than the rotation period of the "atmosphere," yields a good approximation to a true zonal average obtained with regularly spaced data. The errors in the mean quantities thus depend on the errors incurred in making the individual measurements. There are several sources of error that affect the outcome of a single measurement of cloud velocity. These include the estimable errors, such as navigation errors, random errors in measuring cloud displacements, etc., and the intangible errors, such as the ones introduced by total misidentification of a target cloud in the succeeding image of an image pair due to misperception on the part of the operator.

While the errors in data navigation introduce systematic errors in the velocity measurements made on a given image pair, it introduces over the entire set of images a random error in the measurements, and is expected to average out. On the other hand, the errors introduced by erroneous cloud identification may not always be random and may introduce systematic errors in the mean quantities. There is no easy procedure to estimate this error in a reasonable manner except by using different operators in making the measurements, as is done in the present study. It appears unlikely, although not impossible, that different operators would have similar biases in making the measurements, and thus the differences in the mean quantities as deter-

mined from independent samples is a reasonable estimate of the systematic errors.

The image navigation is relatively quite good for the entire sample. This is mainly due to the excellent geometric fidelity of the spin-scan imaging technique used by the OCPP. Typical navigation errors amount to no more than one image element over most of each full-disk image. This corresponds to approximately 25 km at the image center. Considering that the nominal time difference between two successive images used for cloud tracking is somewhat greater than 4 hr, the uncertainty in individual velocity measurements amounts to about 3 m/sec. Gradual changes in the spacecraft spin rate and attitude during the acquisition of a given image may introduce smaller errors in the absolute navigation, and these are generously estimated to be less than 2 m/sec. All the cloud coordinates are determined in a Venus-centered coordinate frame that rotates once every 243 days. The  $z$  axis of this coordinate system is taken to be along the spin axis of the solid planet.

The positive spin axis of Venus is assumed to be that specified by the Pioneer Venus Project Office (Document No. PT-400, National Aeronautics and Space Administration, Ames Research Center, Moffett Field, Calif.) and is at  $-89.0^\circ$  celestial latitude and  $157.0^\circ$  celestial longitude, or  $272.8^\circ$  right ascension and  $66.2^\circ$  declination. This location is very close to the 1970 IAU adopted location although subsequent observations have warranted a new location at  $-88.4^\circ$  right ascension and  $67.3^\circ$  declination (Davies *et al.*, 1980). The impact of a new spin location is most noticeable in the meridional component of motion as an offset of about 1 m/sec and is hardly noticeable in the zonal component of motion.

The quality of each image navigation was carefully examined before reformatting the raw OCPP data into latitude-longitude maps by generating a latitude and longitude grid overlay for the raw data and comparing the predicted planet limb position with the observed limb position. The fit was usually

good to within one image element or scan line over most of the image. We estimate the total uncertainty due to navigation errors and limiting resolution of the data to be approximately 5 m/sec in a single measurement of a cloud velocity. Zonal averaging of the measurements substantially reduces the effect of this error in the mean values, amounting to about 1 m/sec for the zonal and somewhat less for the meridional component between 20° north and 35° south latitudes. At other latitudes the estimated errors in the sample mean values  $\langle u \rangle$  and  $\langle v \rangle$  are larger. These uncertainty estimates do not include any effects of systematic tracking errors that may not be averaged out as discussed earlier.

By looking at several images used in cloud tracking and noting the significant changes in the cloud patterns, we estimate that the errors introduced by misidentification of a target cloud may be as large as 10 to 20 m/sec in some instances. In view of the somewhat different morphology and evolution of the ultraviolet cloud features on Venus at different latitudes, we may expect the error introduced in the measured cloud velocities by misidentification to be variable with latitude. Due to the absence of any images in the intervening time, it is not possible to estimate this error with reliability and we depend on the agreement between independent measurements to provide us with an estimate of the error in the zonal mean circulation due to this source.

Another point that needs to be mentioned here is that the latitudinal sampling of vectors is not uniform in the manual tracking, and is best in low latitudes where a greater number of trackable features are seen on the disk of Venus and fewer at higher latitudes. As a means of estimating the reliability of the sample means, the standard error of the mean (given by the standard deviation of the sample divided by the square root of the number of points) is used to estimate limits within which the two data sets may be expected to agree in the presence of random errors only. Any differences larger

than the expected errors then reflect the systematic errors.

## 5. THE CLOUD MOTION VECTORS

The two sets of measurements yielded samples of approximately 3900 and 3600 vectors each. The latitudinal and longitudinal distribution of the vectors in the two sets was roughly similar and showed no regions of preferred sampling. The latitudinal sampling for both the data sets is presented in Fig. 1.

Normal meteorological notation is used in describing the measurements in this paper, and is as follows:  $u$  and  $v$  denote the zonal and meridional components of motion of individual clouds. Subscripts 1 and 2, when they appear after  $u$  or  $v$ , denote the first and the second vectors obtained by following a cloud in three successive images. Brackets imply zonal as well as temporal averaging, and primes denote deviations or eddies from the mean values obtained. No effort is made to separate the time and zonal means and transient and stationary eddies.

When the time period between successive images of a triplet is small, comparison of the two vectors obtained by following a single cloud in all three images is a useful measure of the errors of navigation if other errors are small. In view of the relatively long interval between the first image and the third image of a triplet, the differences between the first and the second vector are likely to be real and represent spatial and temporal accelerations. In view of the likely presence of planetary-scale waves, we suspect that the spatial accelerations would be greater than the temporal accelerations over the span of three images (roughly 15 hr). The vector pair differences for the two sets are remarkably similar. Further, the ensemble averages for the component differences for the same clouds are about  $-5$  and  $-6$  m/sec for the  $u$  component and about 1 and 2.6 m/sec for the  $v$

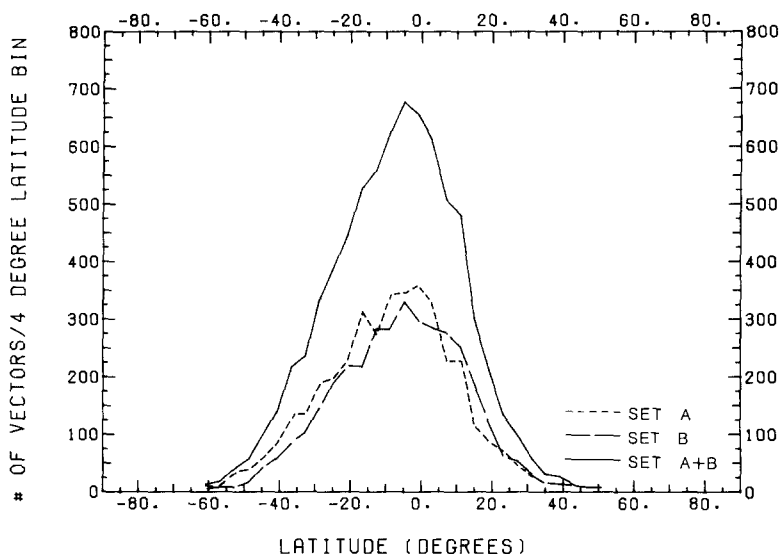


FIG. 1. Number of vectors in each 4°-wide latitude bin for sets A and B, separately and together.

component for observation sets A and B, respectively. The standard error estimates for these differences are less than 1 m/sec. Thus within the expected errors, the  $v$  component shows little change over a triplet, whereas the  $u$  component difference, which on the average shows faster  $u_2$  values, is likely to be real. Note that in all the images the clouds are seen to move from the morning terminator, toward the subsolar point. If the  $u$  component difference for the pair of vectors obtained from triplets is real, then it is a likely manifestation of some solar influence on the cloud motions. Mariner 10 data also showed a similar acceleration of clouds as they moved from the morning region toward the afternoon region on Venus.

## 6. MEAN CIRCULATION

The vectors are binned into 4°-wide latitude bins and averaged to yield zonal means of the zonal and meridional components of motion. The average values are assigned to the average latitude of all the observations in each latitude bin.

The meridional momentum transports by

the zonal mean circulation,  $\langle u \rangle \langle v \rangle$ , and by the eddy circulation,  $\langle u'v' \rangle$ , were also calculated for each latitude bin. The eddy components in the zonal and the meridional directions are determined relative to the respective mean values obtained from the present observations only, and as such the calculated eddy momentum transports  $\langle u'v' \rangle$  are expected to be representative of the present observation period only. These eddy momentum transport estimates are likely to be different if long-term mean values of the latitudinal profiles of the zonal and the meridional components are used, in view of the apparent variability of the zonal circulation at the cloud top level on Venus. Until the validity of these estimates is established further, caution is warranted in their interpretation. The results are summarized in Tables II and III for data sets A and B analyzed independently, and in Table IV for sets A and B analyzed together as a single set. Along with zonal average values, the tables also list root mean square (rms) deviation, standard error (defined as rms deviation divided by the square root of the number of samples in a latitude bin) of  $\langle u \rangle$ ,

TABLE II  
ZONAL MEAN STATISTICS FOR SET A

(Lat) (deg.)	$\langle u \rangle$	$\langle v \rangle$	rms $u$	rms $v$	$Eu$	$Ev$	$\langle u \rangle \langle v \rangle$	$\langle u'v' \rangle$	rms	$E$	Omega (rad/day)	$P$ (days)	$N$
	m/sec						(m/sec) <sup>2</sup>						
39.0	-86.5	8.4	16.0	7.4	4.5	2.1	-727.1	-47.6	125.7	34.9	-1.57	4.00	13
34.7	-90.7	8.6	14.0	6.8	3.6	1.8	-781.4	-48.6	174.0	44.9	-1.56	4.03	15
31.0	-86.9	7.0	16.5	9.3	3.1	1.8	-605.1	-68.8	156.3	29.5	-1.43	4.39	28
27.1	-88.8	7.0	16.0	6.6	2.4	1.0	-617.5	-63.4	119.7	17.8	-1.41	4.46	45
23.1	-100.2	8.5	13.5	9.2	1.6	1.1	-847.4	-64.0	189.3	22.5	-1.54	4.09	71
19.0	-93.7	4.9	16.2	8.9	1.7	0.9	-456.2	-83.0	213.8	22.8	-1.40	4.49	88
14.8	-97.2	4.3	19.3	8.5	1.8	0.8	-416.4	-62.5	217.4	20.2	-1.42	4.43	116
11.1	-94.6	2.4	14.8	6.3	1.0	0.4	-223.4	-31.8	125.3	8.3	-1.36	4.62	228
6.9	-94.1	1.8	16.8	6.5	1.1	0.4	-167.2	-3.3	136.7	9.0	-1.34	4.70	229
2.7	-95.5	1.4	15.8	5.5	0.9	0.3	-133.0	-7.1	130.6	7.2	-1.35	4.66	330
-1.1	-92.9	1.6	17.1	5.7	0.9	0.3	-148.3	12.8	131.6	7.0	-1.31	4.79	358
-4.8	-93.8	-0.1	15.1	5.8	0.8	0.3	7.0	12.4	118.9	6.4	-1.33	4.73	346
-8.9	-96.2	-1.1	16.1	5.5	0.9	0.3	108.2	23.3	96.8	5.2	-1.37	4.57	341
-13.0	-94.1	-0.5	16.0	7.0	1.0	0.4	44.5	8.3	161.1	9.8	-1.36	4.61	273
-16.7	-89.6	-2.3	15.5	6.0	0.9	0.3	206.3	21.1	110.6	6.3	-1.32	4.76	310
-20.9	-91.3	-3.1	15.2	6.6	1.0	0.4	280.2	33.2	107.3	7.1	-1.38	4.56	226
-24.9	-92.1	-4.6	16.2	6.9	1.2	0.5	424.2	22.1	132.6	9.4	-1.43	4.38	197
-28.7	-88.5	-4.6	16.4	6.7	1.2	0.5	407.4	52.7	124.3	9.1	-1.43	4.41	188
-32.9	-86.1	-4.9	16.5	7.1	1.4	0.6	426.0	43.9	159.5	13.7	-1.45	4.34	135
-36.8	-84.9	-5.3	15.3	6.7	1.3	0.6	448.8	48.3	126.9	11.0	-1.50	4.20	134
-41.0	-82.5	-6.7	18.9	8.3	2.1	0.9	554.8	73.7	181.0	20.0	-1.54	4.07	82
-44.8	-71.6	-6.0	20.1	9.1	2.6	1.2	431.1	41.2	218.5	28.7	-1.42	4.41	58
-49.0	-71.4	-8.1	16.7	7.6	2.7	1.2	577.1	59.0	140.6	22.5	-1.53	4.09	39
-52.4	-57.9	-5.4	14.9	6.4	2.5	1.1	313.9	52.0	91.2	15.4	-1.34	4.69	35
-56.7	-59.1	-5.9	16.2	5.3	5.1	1.7	350.0	-18.1	134.2	42.4	-1.52	4.13	10
-61.0	-46.3	-1.7	6.2	2.8	2.1	0.9	79.1	6.3	16.6	5.5	-1.35	4.66	9

*Note.* (Lat): Average latitude of the observations.  $\langle u \rangle$ : Average zonal component of motion.  $\langle v \rangle$ : Average meridional component of motion. rms  $u$ : Root mean square deviation about  $\langle u \rangle$ . rms  $v$ : Root mean square deviation about  $\langle v \rangle$ .  $Eu$ : Standard error of  $\langle u \rangle$  given by rms  $u$ /sqr  $t(N)$ .  $Ev$ : Standard error of  $\langle v \rangle$  given by rms  $v$ /sqr  $t(N)$ .  $\langle u \rangle \langle v \rangle$ : Meridional momentum transport by the mean circulation.  $\langle u'v' \rangle$ : Meridional momentum transport by the eddy circulation. rms: Standard deviation about  $\langle u'v' \rangle$ .  $E$ : Standard error of  $\langle u'v' \rangle$  given by rms  $\langle u'v' \rangle$ /sqr  $t(N)$ . Omega: Angular velocity in radians per day.  $P$ : Period of rotation corresponding to Omega, in days.  $N$ : Number of vectors in a given latitude bin.

$\langle v \rangle$ , and  $\langle u'v' \rangle$ , and the momentum transports, the angular velocity, and the period of rotation for the corresponding mean zonal component of motion. We emphasize here once again that the standard error calculated here is presented solely to seek limits within which the two sets of measurements may be expected to agree, and do NOT indicate true uncertainties in the zonal mean quantities presented. The mag-

nitude of the uncertainties in the zonal mean quantities presented is better indicated by the discrepancy between the two data sets, and they are generally much larger than the standard errors of either data set.

#### a. Mean Zonal Component of Motion

Figure 2a shows the zonal mean  $u$  component of motion for set A and B analyzed



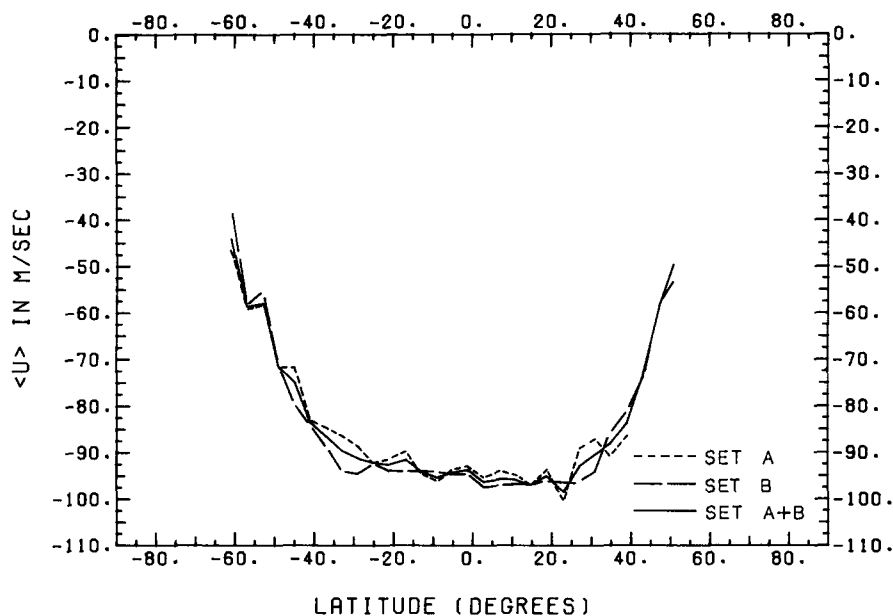
separately as well as together. Figure 2b shows the corresponding rotation period profile. At most latitudes, except between about 30 and 35° south latitude and between 25 and 35° north latitude, the agreement between the  $\langle u \rangle$  profiles for set A and set B is remarkable.

The three curves for the zonal mean  $u$  component have similar rms deviations as well as standard errors, as shown in Figs. 3a and b, respectively, with set A, which was obtained by two operators with the limited display abilities mentioned earlier, showing somewhat larger rms deviations.

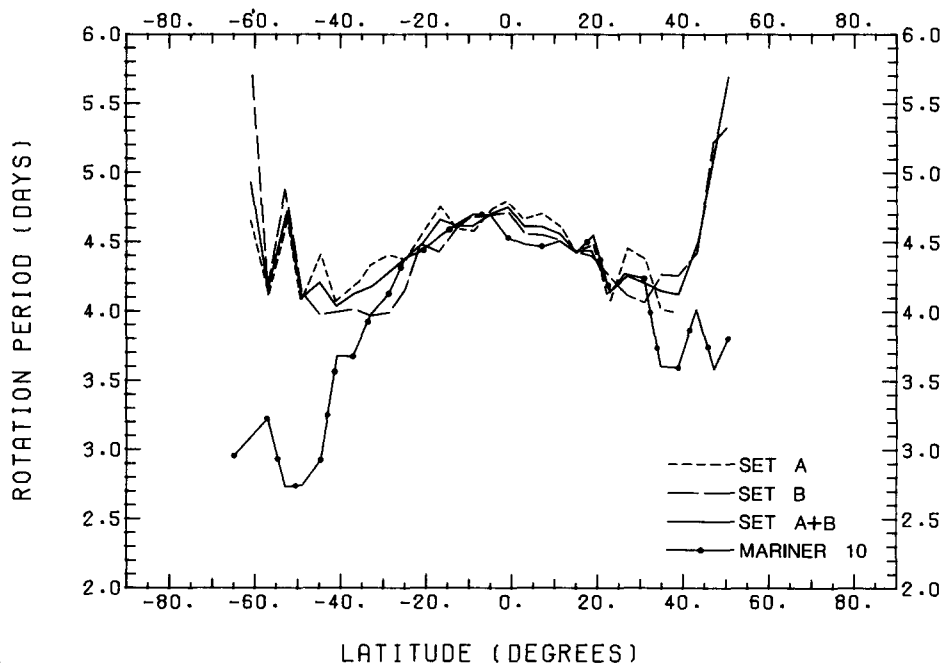
The rms deviations in each latitude bin about the mean zonal component are typically around 15 m/sec, smaller than the standard deviations of about 25 m/sec for the digitally tracked vectors presented by Rossow *et al.* Note that the rms deviation in each latitude bin is due to a combination of measurement errors as well as real variation of the zonal component of motion over time as well as in the longitudinal direction. Unfortunately it is not possible to separate their relative contributions in a direct manner. The discrepancy in the rms deviations for set A and set B is also indicative of the

TABLE III  
ZONAL MEAN STATISTICS FOR MEASUREMENT SET B

(Lat (deg.)	$\langle u \rangle$	$\langle v \rangle$	rms $u$	rms $v$	$Eu$	$Ev$	$\langle u \rangle \langle v \rangle$	$\langle u'v' \rangle$	rms	$E$	Omega (rad/day)	$P$ (days)	$N$
	m/sec						(m/sec) <sup>2</sup>						
50.4	-53.2	10.5	6.6	9.1	3.0	4.1	-555.9	-45.6	85.0	38.0	-1.18	5.33	5
47.3	-57.8	9.5	12.7	6.7	5.2	2.7	-550.7	-9.3	56.1	22.9	-1.20	5.22	6
43.3	-73.1	10.8	12.1	5.3	3.8	1.7	-793.6	-5.4	28.8	9.1	-1.42	4.43	10
39.1	-80.9	8.7	15.6	7.1	4.3	2.0	-705.6	-79.9	142.3	39.5	-1.47	4.27	13
34.9	-85.6	9.6	12.4	7.5	3.1	1.9	-818.1	-17.2	123.3	30.8	-1.47	4.27	16
31.1	-93.7	11.7	16.4	7.6	3.0	1.4	-1100.3	-47.2	114.9	21.0	-1.54	4.07	30
27.0	-96.1	9.8	13.4	5.6	1.8	0.8	-938.3	-39.9	92.6	12.7	-1.52	4.13	53
23.1	-96.4	10.9	13.1	7.1	1.7	0.9	-1050.9	-58.2	161.1	20.5	-1.48	4.25	62
18.6	-95.8	8.5	12.4	5.6	1.1	0.5	-811.1	-20.9	104.5	9.3	-1.43	4.41	127
15.0	-96.8	7.3	11.0	5.2	0.8	0.4	-704.6	-4.1	64.9	4.8	-1.41	4.44	183
11.0	-96.5	6.3	11.3	5.0	0.7	0.3	-610.2	-1.6	51.0	3.2	-1.39	4.53	251
7.1	-96.8	4.2	12.6	4.5	0.8	0.3	-404.9	-0.5	61.6	3.7	-1.38	4.56	274
3.2	-97.3	3.2	11.0	4.9	0.7	0.3	-309.3	-1.9	62.6	3.7	-1.38	4.57	283
-0.9	-94.4	3.0	10.9	4.9	0.6	0.3	-280.7	2.1	70.0	4.1	-1.33	4.72	297
-4.8	-94.4	0.3	11.4	4.7	0.6	0.3	-28.4	-0.9	57.6	3.2	-1.34	4.70	329
-9.0	94.0	-0.4	11.5	5.0	0.7	0.3	41.0	6.5	58.1	3.5	-1.34	4.68	282
-12.9	-93.8	-1.4	11.7	4.7	0.7	0.3	130.4	10.3	59.1	3.5	-1.36	4.63	283
-16.9	-93.8	-3.4	12.5	6.4	0.9	0.4	316.2	23.7	93.5	6.4	-1.38	4.54	216
-20.8	-93.7	-3.7	10.5	6.0	0.7	0.4	343.1	24.6	101.0	6.8	-1.42	4.44	219
-25.1	-92.1	-4.5	11.8	5.9	0.9	0.4	415.6	25.3	83.4	6.1	-1.44	4.38	189
-28.7	-94.4	-5.5	12.1	6.7	1.0	0.6	523.0	50.5	193.3	15.9	-1.52	4.13	148
-32.9	-93.8	-7.5	13.8	5.6	1.4	0.6	700.7	24.8	67.9	6.7	-1.58	3.98	102
-36.7	-88.8	-6.7	15.7	7.4	1.7	0.8	591.0	40.6	123.5	13.5	-1.56	4.02	84
-40.8	-84.2	-7.6	19.3	6.5	2.5	0.8	639.1	65.1	155.7	20.4	-1.57	4.00	58
-44.8	-79.4	-7.0	18.8	6.0	2.9	0.9	552.3	57.2	120.2	18.8	-1.58	3.98	41
-48.8	-70.9	-7.2	14.4	6.1	3.5	1.5	511.2	55.0	112.6	27.3	-1.52	4.14	17
-52.9	-55.1	-6.9	10.6	6.7	4.0	2.5	380.9	-15.5	68.0	25.7	-1.29	4.88	7
-57.1	-58.1	-8.3	16.5	3.0	5.8	1.1	482.2	7.2	61.7	21.8	-1.51	4.17	8
-60.6	-38.3	-1.5	6.2	4.5	3.1	2.3	56.1	15.8	31.5	15.8	-1.10	5.71	4

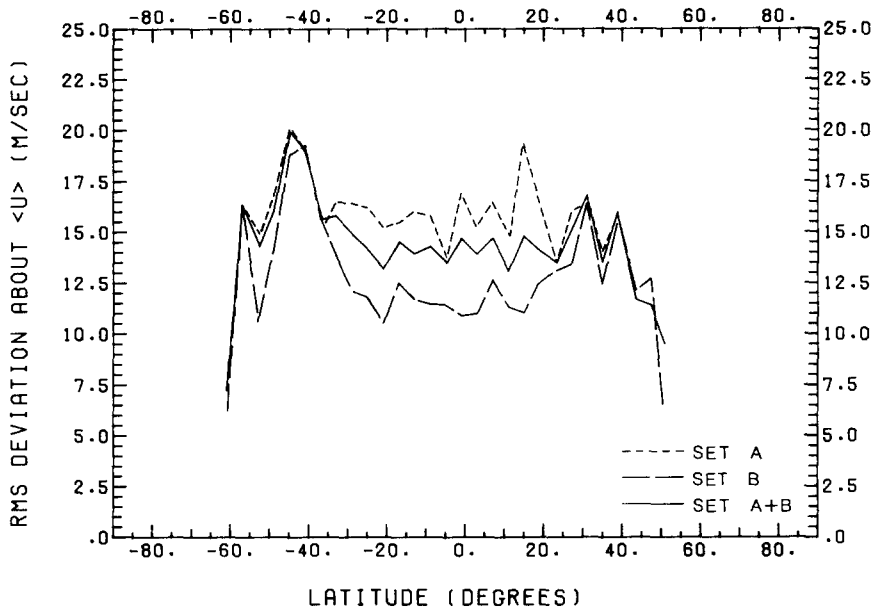


a

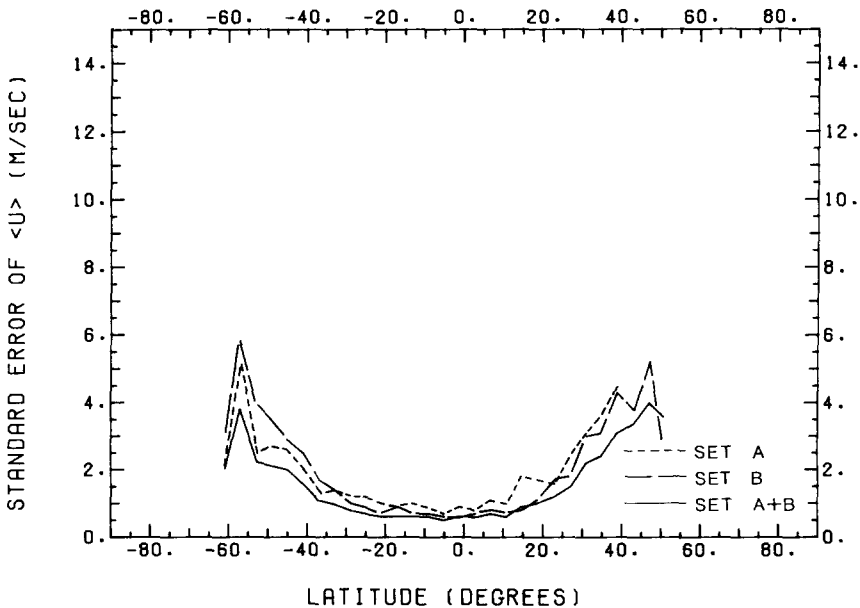


b

FIG. 2. Latitudinal profile of (a) the mean zonal component of motion for the three cases (sets A and B separately, and analyzed together) and (b) corresponding rotation periods in days.



a



b

FIG. 3. Latitudinal profile of (a) rms deviation about  $\langle u \rangle$  (b) standard error of  $\langle u \rangle$ , both for the three cases analyzed, and (c) difference of the  $\langle u \rangle$  profiles of set A and set B.

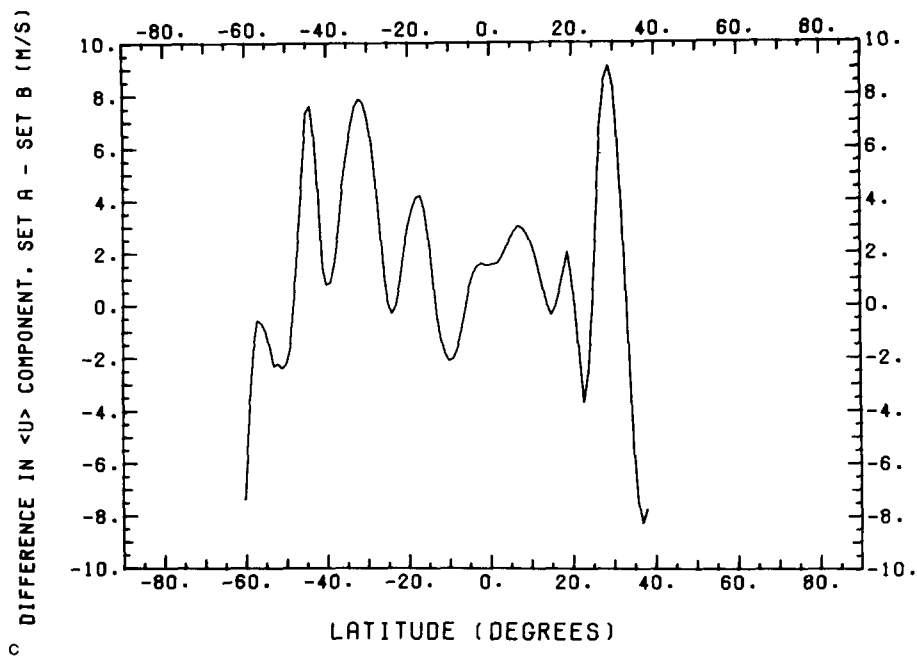


FIG. 3—Continued.

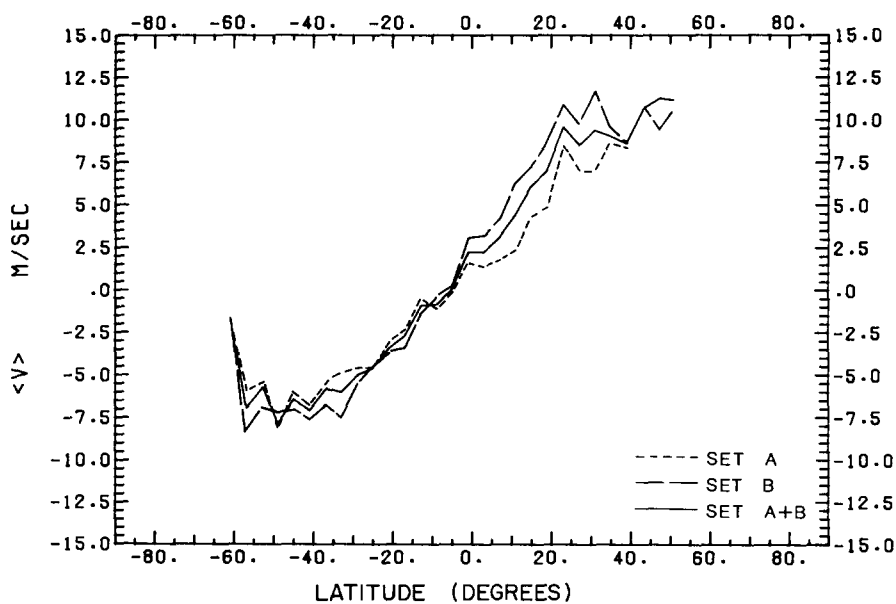


FIG. 4. Mean meridional component of motion,  $\langle v \rangle$ , as a function of latitude for the three cases.

significant measurement errors. Nevertheless, the magnitude of the rms deviations may be taken to be the upper limit on the spatial and temporal variability of the zonal component of motion for the data analyzed. Between 20° north and 35° south latitudes the estimated standard error of the zonal mean component  $\langle u \rangle$  for both sets is about 1 m/sec. As mentioned earlier, this simply indicates that a reasonable number of vectors have been obtained for a given latitude, so that the mean value is stable, and not the true error in the actual mean zonal component. It is thus interesting to look at the actual differences in the two estimates of  $\langle u \rangle$  profile (Fig. 3c). As is apparent, the differences are smaller than 4 m/sec between 30° south and about 22° north latitudes, and much higher outside this region, approaching 8 m/sec at 30° north and 42° south latitudes. The larger differences at these higher latitudes appear related to the relatively poorer sampling of cloud motion vectors at those latitudes, although some systematic bias may also be present. These differences are thus more indicative of true uncertainty in the zonal mean profile obtained in this study. In subsequent analysis, the zonal means obtained by adding the two sets are considered our best estimate in view of the general agreement between the two sets, with the uncertainty in the mean quantities thus obtained being approximately given by the differences between the results of the two measurement sets analyzed independently. The profiles shown in Fig. 2a are close to that presented by Rossow *et al.* (1980) from digital tracking, although the present profile appears to be somewhat faster by 2 to 5 m/sec at most latitudes. Between 30° south and 20° north the differences are less than 5 m/sec. These differences are thus further indications of the uncertainty in the true zonal mean component profile. Note also that the manual vectors analyzed here cover a somewhat longer period than the images from which the results of Rossow *et al.* were obtained.

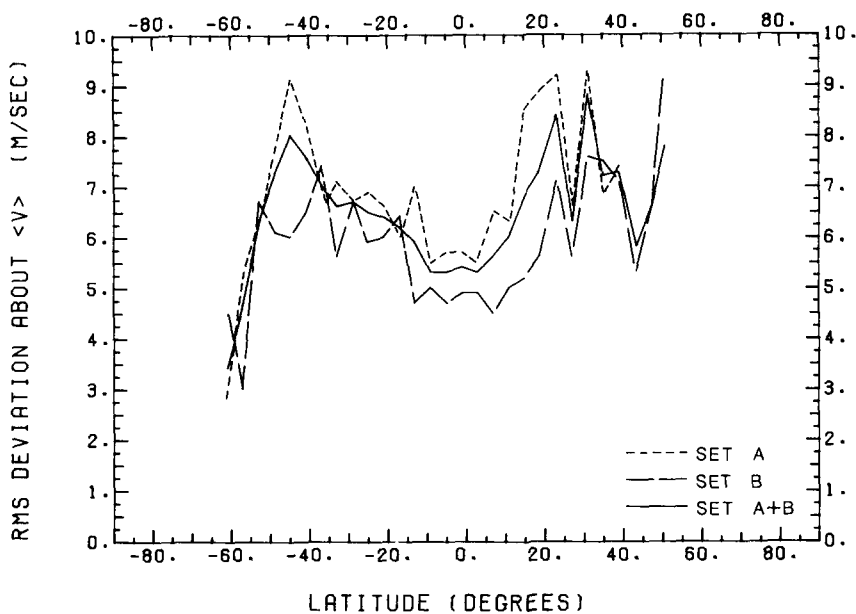
Although the  $\langle u \rangle$  is devoid of high-speed

jets in midlatitudes the atmospheric rotation period profile corresponding to  $\langle u \rangle$  shows weak jets, as can be seen in Fig. 2b. The departure from a rigid body rotation of the atmosphere at the cloud top level is definitely indicated by the shape of the angular velocity profile. Mariner 10 jets showed peak angular velocities much higher than that in the present case corresponding to a rotation period of only about 2.8 days rather than 4.2 days, as can be seen in this figure.

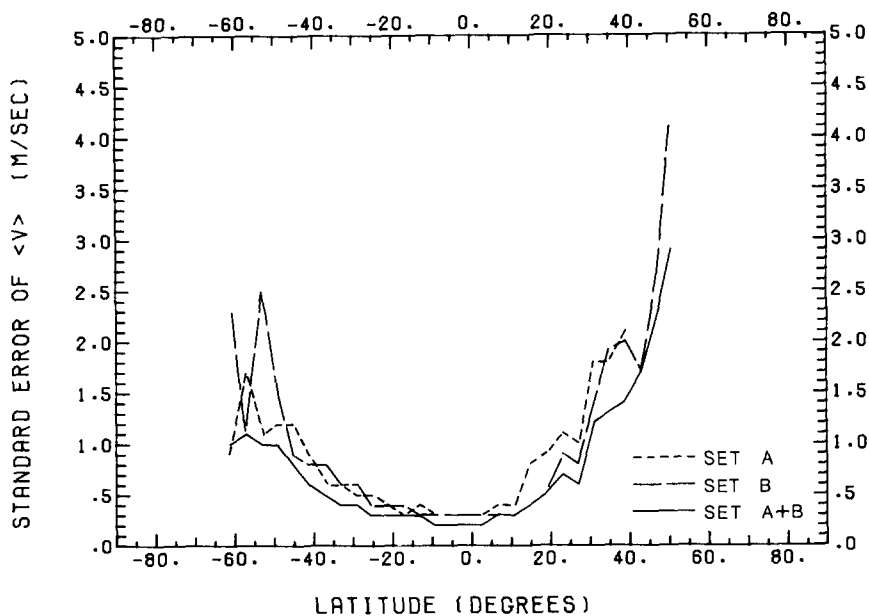
#### *b. Mean Meridional Component of Motion*

Figure 4 shows the mean meridional component of motion for the three cases. Once again, the agreement between the two sets of measurements is remarkable. Further, these profiles are quite similar in shape and magnitude to the profile presented by Rossow *et al.* (1980). The mean meridional component of motion is directed toward the pole in either hemisphere, except between the equator and about 5° south latitude, where the flow is toward the equator. This peculiar bias was also seen in the Mariner 10 observations (Limaye and Suomi, 1981) but the change in direction was at a more southerly latitude. However, a large part of this apparent asymmetry is removed if the newer Venus spin axis location is used for decomposing the measured cloud motion vectors into zonal and meridional components.

The rms deviation about the mean meridional component typically is only about half as large as that for the zonal component at most latitudes, and is shown in Fig. 5a for the three cases. Also shown in Fig. 5b are the corresponding estimates of standard error of  $\langle v \rangle$ . At most latitudes the errors are small, thereby indicating adequate sampling as far as the meridional component is concerned. The differences in the  $\langle v \rangle$  profiles, which, like the differences in the  $\langle u \rangle$  profiles for the two sets, indicate the true uncertainty in the mean meridional component, are shown in Fig. 5c.



a



b

FIG. 5. (a) rms deviation about  $\langle v \rangle$  for each latitude bin for the three cases analyzed, (b) corresponding standard error of  $\langle v \rangle$ , and (c) the difference between the  $\langle v \rangle$  profiles obtained from set A and set B.

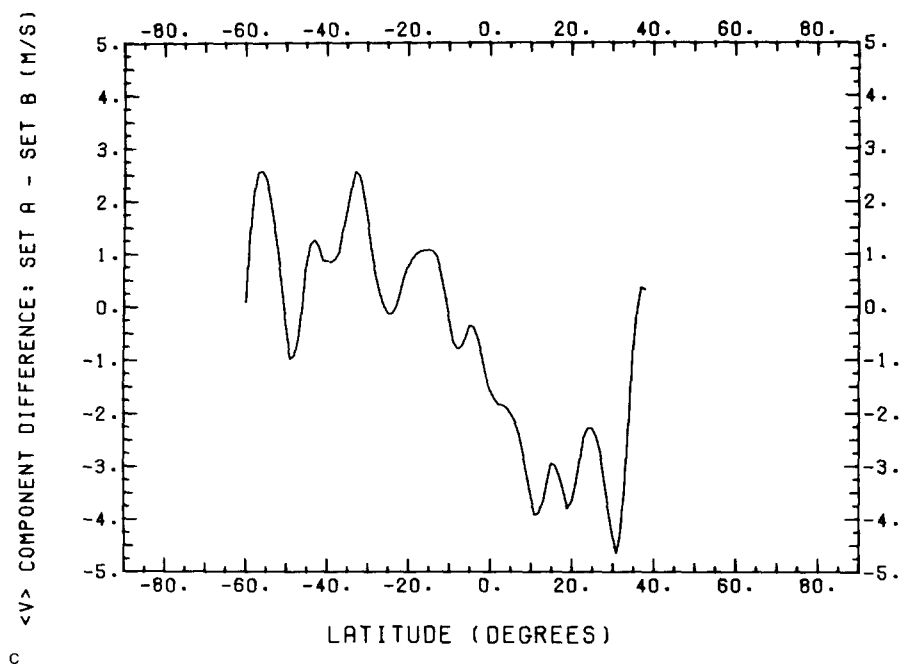


FIG. 5—Continued.

The comments made about the rms deviation about  $\langle u \rangle$  also apply to the rms deviation about  $\langle v \rangle$  in a given latitude bin. Thus the calculated rms deviation is indicative of true variability of the meridional component in space and time as well as of measurement errors. The fact that the rms deviation for the meridional component is smaller than that for the zonal component may be due to a relatively larger variation in the mean zonal component with time (see below). This could also be due to larger errors in the  $u$  component measurements or larger eddy components in the zonal components or both; however, it is not clear whether this is indeed the case. Long-term variability of the mean zonal component is partially borne out by differences in the spring and fall data as described below.

Figure 5c shows that the differences between the two estimates of the  $\langle v \rangle$  profile are greater than the standard errors of the two sets at many latitudes. These differences are thus indicative of the uncertainty in the estimate obtained by analyzing sets A

and B together, similar to the  $\langle u \rangle$  component, and have peak magnitudes of about 3 m/sec in the southern hemisphere and 4 m/sec in the northern hemisphere.

### c. Meridional Momentum Transports

The meridional transport of momentum in an atmosphere is an important diagnostic quantity. At the cloud top levels in the Venus atmosphere the zonal mean circulation shows either a broad equatorial jet in terms of the zonal component of motion, as in the present case, or a pair of midlatitude jets in either hemisphere as in the Mariner 10 observations. The processes that maintain these jets, or rather the processes that are responsible for the growth and decay of these variable jets, are not yet fully understood although several suggestions have been made (Gierasch, 1975; Rossow and Williams, 1979; Rossow *et al.*, 1980). All of these suggested mechanisms for the super-rotation of the Venus atmosphere and the midlatitude jets invoke interplay between the meridional transport of momentum by

the mean circulation and by the eddy circulation. Eddy activity at the cloud level in the Venus atmosphere is indicated by cloud brightness spectra and cloud motions themselves (Belton *et al.*, 1976; Limaye, 1977; Limaye and Suomi, 1981; Travis, 1978; Rossow *et al.*, 1980; Del Genio and Rossow, 1982) and is suggested by theoretical investigations (Rossow and Williams, 1979; Covey and Schubert, 1981). It is thus of considerable interest to estimate the mean and eddy circulation momentum transports. However, the calculation of the eddy momentum transports is a difficult task in view of the relatively limited amount of data, the significant uncertainties in the mean profiles of  $\langle u \rangle$  and  $\langle v \rangle$ , and the apparent variability of the "mean" circulation as determined from short periods of observations. Nevertheless, some useful information may be obtained by calculating these transports from the present data until more observations are available. Limaye and Suomi (1981) have presented some rough estimates of these transports for the Mariner 10 observations when there was a midlatitude jet present in either hemisphere, and in view of the absence of the midlatitude jets in the Pioneer Venus data a comparison is warranted.

The meridional transports of momentum by the mean circulation,  $\langle u \rangle \langle v \rangle$ , and that by the eddy circulation,  $\langle u'v' \rangle$ , obtained from the cloud motion measurements are presented in Figs. 6a and b, respectively. The eddy components of the zonal and meridional components of motion are obtained as departures from the mean values  $\langle u \rangle$  and  $\langle v \rangle$  obtained from all the vectors lying in a given latitude bin. No allowance is made for the variation of the mean components over the width of the bin. Inclusion of this slight variation changes the eddy estimates by a negligible amount. The poleward momentum transport by the horizontal eddies is then the covariance  $\langle u'v' \rangle$  which is calculable in a straightforward manner.

To estimate the reliability of eddy momentum transports in each latitude bin,

both the rms deviation and the standard error of  $\langle u'v' \rangle$  were calculated in each bin. Both of these quantities are shown as a function of latitude in Figs. 7a and b for the three cases studied. The rms deviation about  $\langle u'v' \rangle$  gives an indication of the variability of the magnitudes of the eddy components in a latitude bin, while the corresponding standard error shows the stability of the estimated mean covariance  $\langle u'v' \rangle$  in view of the large deviations and limited data. Once again, it is emphasized that the standard error of  $\langle u'v' \rangle$  is presented only as limits within which the two estimates from sets A and B may be expected to agree, and not as true error in the eddy momentum transport which is likely to be much higher. Just as in the case of the zonal mean  $u$  and  $v$  components of motion, the true uncertainties in the mean and eddy circulation transports are perhaps better indicated by the differences between the results for the two sets of measurements, which theoretically are expected to be identical. As can be seen from the results presented, these differences in the estimates of momentum transport are large, but qualitatively the results are similar.

In view of the up to 8 m/sec uncertainty in the  $\langle u \rangle$  component and about 4 m/sec in the  $\langle v \rangle$  component magnitude, the actual uncertainty in the mean circulation momentum transport may be as high as 400 (m/sec)<sup>2</sup> polewards of 20° latitude in either hemisphere as is indicated by the differences in the  $\langle u \rangle \langle v \rangle$  profiles for set A and for set B in the northern hemisphere (Fig. 6a).

In qualitative agreement with the Mariner 10 results presented by Limaye and Suomi (1981), the mean circulation momentum transport appears to dominate that by the eddy circulation at the latitudes observed. The transports by the circulations do appear to be generally in the same sense at most latitudes. The qualitative similarity between the Mariner 10 estimates and the present estimates may only be a coincidence. One certainly would not have expected them to be similar in view of the



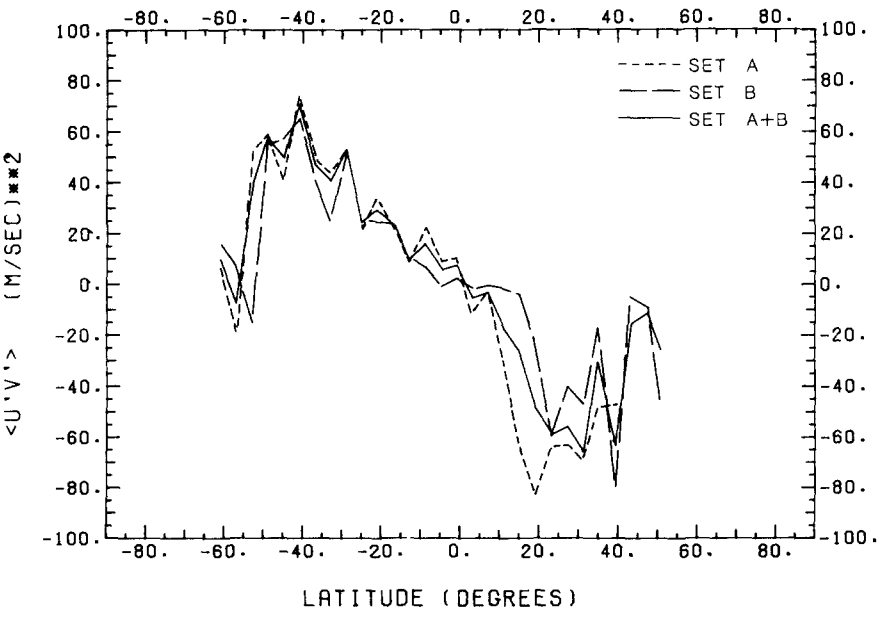
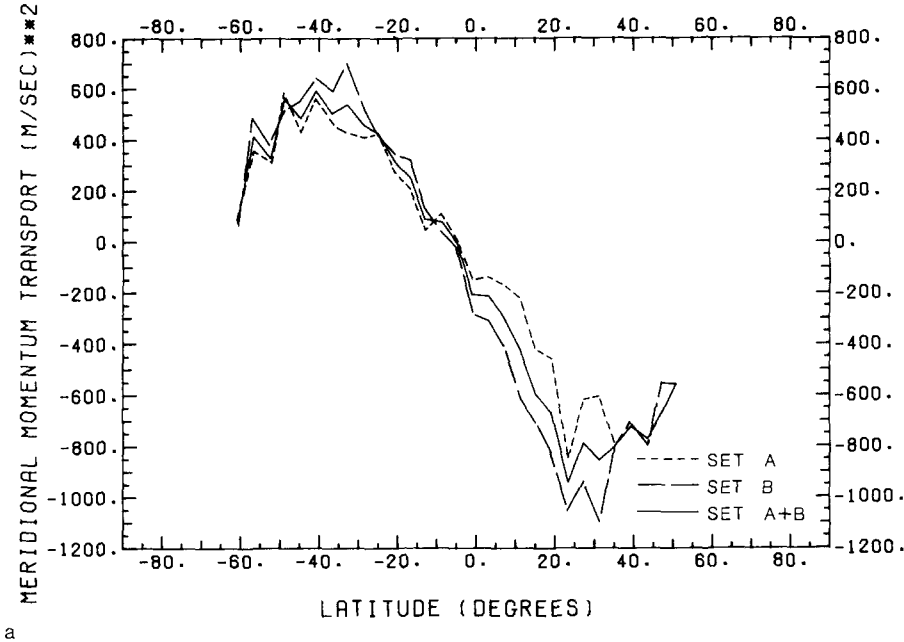
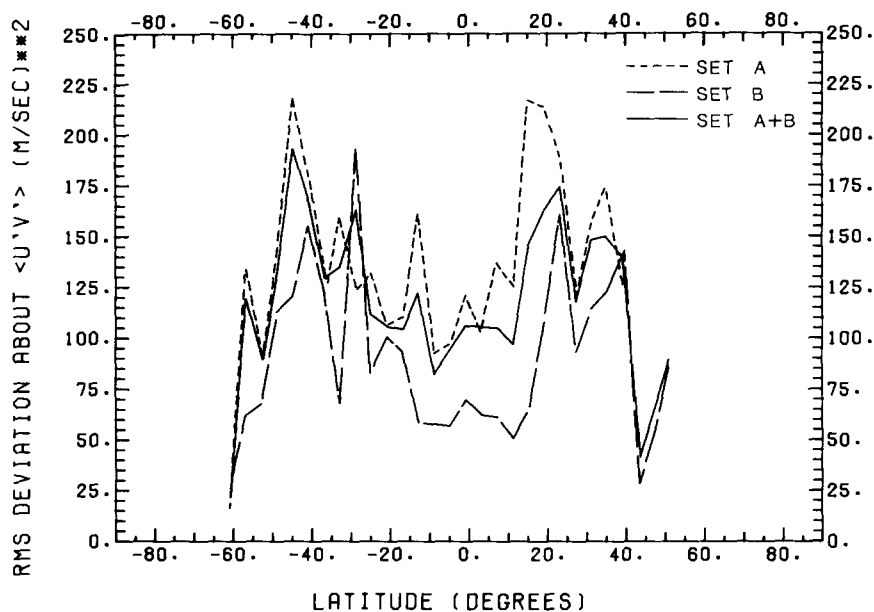
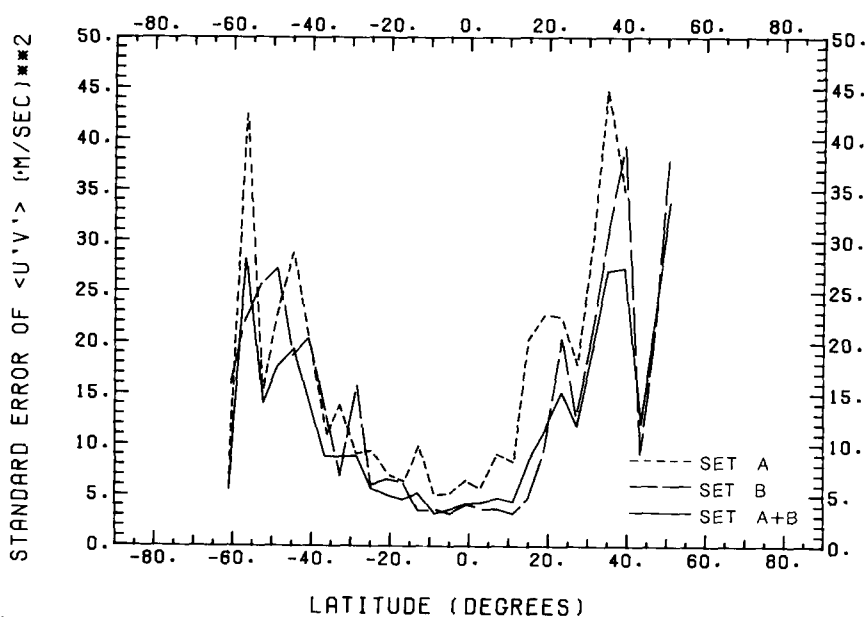


FIG. 6. Contribution to the meridional momentum transport by (a) the mean circulation,  $\langle u \rangle \langle v \rangle$ , as a function of latitude, and (b) by the eddy circulation,  $\langle u'v' \rangle$ . Both figures show results for the three cases analyzed.



a



b

FIG. 7. (a) rms deviation about  $\langle u'v' \rangle$  in each latitude bin, and (b) corresponding standard error of  $\langle u'v' \rangle$ .

different meridional profiles of  $\langle u \rangle$ . They may, however, be consistent if the Mariner 10 and Pioneer Venus observations refer to specific phases in the growth and decay

phases of the midlatitude jets as discussed by Rossow *et al.* (1980).

Despite the large uncertainties in both the mean and eddy momentum transports it

TABLE IV  
ZONAL MEAN STATISTICS FOR SETS A AND B COMBINED

(Lat) (deg.)	$\langle u \rangle$	$\langle v \rangle$	rms $u$	rms $v$	$Eu$	$Ev$	$\langle u \rangle \langle v \rangle$	$\langle u'v' \rangle$	rms	$E$	Omega (rad/day)	$P$ (days)	$N$
	m/sec						(m/sec) <sup>2</sup>						
50.7	-49.5	11.2	9.5	7.8	3.6	2.9	-555.8	-26.1	89.5	33.8	-1.10	5.70	7
47.3	-58.5	11.3	11.4	6.6	4.0	2.3	-662.8	-11.4	67.5	23.9	-1.22	5.16	8
43.3	-72.2	10.7	11.7	5.8	3.4	1.7	-771.5	-15.5	42.0	12.1	-1.40	4.49	12
39.0	-83.7	8.6	16.0	7.3	3.1	1.4	-716.8	-63.3	139.3	27.3	-1.52	4.13	26
34.8	-88.1	9.1	13.5	7.2	2.4	1.3	-801.6	-31.2	150.2	27.0	-1.51	4.15	31
31.1	-90.4	9.4	16.8	8.8	2.2	1.2	-853.2	-65.7	148.5	19.5	-1.49	4.22	58
27.1	-92.7	8.5	15.1	6.3	1.5	0.6	-785.9	-55.8	118.0	11.9	-1.47	4.27	98
23.1	-98.4	9.6	13.5	8.4	1.2	0.7	-944.6	-59.0	174.9	15.2	-1.51	4.16	133
18.8	-94.9	7.0	14.1	7.3	1.0	0.5	-664.0	-48.1	162.3	11.1	-1.42	4.44	215
14.9	-96.9	6.1	14.8	6.8	0.9	0.4	-593.1	-26.4	145.2	8.4	-1.42	4.44	299
11.0	-95.6	4.4	13.1	6.0	0.6	0.3	-424.2	-17.8	96.8	4.4	-1.37	4.57	479
7.0	-95.5	3.1	14.7	5.6	0.7	0.3	-295.1	-3.4	105.1	4.7	-1.36	4.62	503
2.9	-96.3	2.2	13.9	5.3	0.6	0.2	-213.6	-5.5	105.6	4.3	-1.36	4.62	613
-1.0	-93.6	2.2	14.7	5.4	0.6	0.2	-207.9	7.5	106.4	4.2	-1.32	4.76	655
-4.8	-94.1	0.1	13.5	5.3	0.5	0.2	-10.2	5.9	94.4	3.6	-1.33	4.71	675
-8.9	-95.2	-0.8	14.3	5.3	0.6	0.2	77.4	16.1	82.5	3.3	-1.36	4.62	623
-13.0	-93.9	-0.9	13.9	5.9	0.6	0.3	88.3	9.2	121.9	5.2	-1.36	4.62	556
-16.8	-91.3	-2.7	14.5	6.2	0.6	0.3	250.4	23.2	104.5	4.6	-1.35	4.67	526
-20.8	-92.5	-3.4	13.2	6.4	0.6	0.3	310.8	29.3	105.7	5.0	-1.40	4.50	445
-25.0	-92.1	-4.6	14.2	6.5	0.7	0.3	420.0	23.7	111.4	5.7	-1.43	4.38	386
-28.7	-91.1	-5.0	14.9	6.7	0.8	0.4	456.9	53.1	164.0	8.9	-1.47	4.28	336
-32.9	-89.4	-6.0	15.8	6.6	1.0	0.4	539.4	40.4	135.4	8.8	-1.50	4.18	237
-36.7	-86.4	-5.8	15.6	7.0	1.1	0.5	502.4	46.6	129.2	8.8	-1.52	4.13	218
-40.9	-83.2	-7.1	19.1	7.6	1.6	0.6	589.4	70.5	169.3	14.3	-1.55	4.04	140
-44.8	-74.8	-6.4	19.9	8.0	2.0	0.8	479.5	49.6	193.7	19.5	-1.49	4.22	99
-48.9	-71.2	-7.8	16.0	7.2	2.1	1.0	557.0	57.9	131.6	17.6	-1.53	4.11	56
-52.5	-57.4	-5.7	14.3	6.5	2.2	1.0	325.7	40.1	90.3	13.9	-1.33	4.72	42
-56.9	-58.6	-7.0	16.3	4.6	3.8	1.1	409.3	-7.5	119.8	28.2	-1.52	4.15	18
-60.9	-43.8	-1.6	7.2	3.4	2.0	1.0	71.6	9.6	21.7	6.0	-1.27	4.94	13

appears that both modes of circulation are generally transporting momentum polewards, with the mean transport being the dominant one. In view of the significant poleward transport of angular momentum one would normally expect a jet structure in the zonal component profile. The absence of such a jet and the lack of any appreciable equatorward export of momentum by the eddy circulation suggest that other mechanisms, such as the vertical exchange of momentum, may be important in the Venus atmosphere, or that the horizontal mixing necessary to create a jet is small so that the time scale for the buildup of a jet from a near solid-body rotation zonal component profile is considerably longer than a

few months (certainly longer than the duration between the two observing periods in 1979 since no significant change is evident in the zonal component profiles for the two periods; see below).

#### *d. Temporal Variability of the Zonal Mean Circulation*

Both the present and Rossow *et al.*'s (1980) estimates of the meridional profile of the mean zonal component at the cloud top level obtained from Pioneer Venus observations during 1979 show a very different structure compared to the circulation seen during the Mariner 10 Venus encounter (Suomi, 1974; Limaye, 1977; Travis, 1978;

TABLE V  
ZONAL MEAN STATISTICS FOR SPRING 1979 DATA

$\langle \text{Lat} \rangle$ (deg.)	$\langle u \rangle$	$\langle v \rangle$	rms $u$	rms $v$	$E u$	$E v$	$\langle u \rangle \langle v \rangle$	$\langle u' v' \rangle$	rms	$E$	Omega (rad/day)	$P$ (days)	$N$
	m/sec						(m/sec) <sup>2</sup>						
50.7	-49.5	10.9	10.3	8.4	4.2	3.4	-537.6	-30.3	99.3	40.5	-1.10	5.70	6
47.5	-57.5	10.5	11.8	6.6	4.5	2.5	-603.5	-6.2	58.7	22.2	-1.20	5.23	7
43.3	-73.1	12.3	12.1	5.0	3.8	1.6	-898.3	-8.3	30.4	9.6	-1.42	4.43	10
39.1	-82.0	7.6	15.5	6.8	3.2	1.4	-625.5	-47.6	119.8	24.5	-1.49	4.22	24
34.9	-86.9	8.4	13.6	7.2	2.7	1.4	-731.2	-39.5	156.8	30.8	-1.50	4.20	26
31.0	-90.3	9.4	17.0	9.0	2.3	1.2	-844.7	-69.8	152.1	20.5	-1.49	4.22	55
27.1	-93.1	8.5	15.2	6.5	1.6	0.7	-793.6	-58.4	122.3	12.8	-1.48	4.26	91
23.0	-99.2	9.7	13.9	8.9	1.3	0.8	-958.3	-65.0	189.2	17.6	-1.52	4.13	115
18.8	-94.9	7.0	14.4	7.5	1.0	0.5	-665.4	-50.8	166.6	11.7	-1.42	4.44	204
14.9	-97.0	6.3	15.0	6.8	0.9	0.4	-607.9	-26.6	147.3	8.7	-1.42	4.43	289
11.0	-95.6	4.3	13.4	6.0	0.6	0.3	-414.8	-18.7	98.8	4.7	-1.38	4.57	449
7.0	-95.4	3.0	15.1	5.5	0.7	0.3	-287.3	-2.4	108.2	5.0	-1.36	4.63	462
2.9	-96.4	2.1	14.3	5.1	0.6	0.2	-201.5	-6.1	108.2	4.5	-1.36	4.61	573
-1.0	-93.8	1.8	15.4	5.4	0.6	0.2	-172.9	7.1	112.8	4.7	-1.32	4.75	577
-4.8	-94.3	-0.2	14.1	5.3	0.6	0.2	22.1	6.0	99.1	4.1	-1.34	4.70	596
-8.9	-95.7	-1.2	14.9	5.2	0.6	0.2	119.4	15.0	84.5	3.6	-1.37	4.59	551
-13.0	-94.5	-1.0	14.8	6.0	0.7	0.3	94.8	8.1	130.4	6.0	-1.37	4.59	474
-16.8	-90.9	-2.8	15.0	6.3	0.7	0.3	252.9	23.6	109.3	5.1	-1.34	4.69	467
-20.8	-93.0	-3.7	13.9	6.5	0.7	0.3	341.7	28.7	112.8	5.9	-1.40	4.47	365
-24.9	-92.1	-4.8	14.7	6.6	0.8	0.4	439.8	24.9	117.4	6.4	-1.43	4.38	332
-28.7	-90.5	-5.2	15.4	7.1	0.9	0.4	474.0	58.2	178.6	10.9	-1.46	4.31	271
-32.9	-88.9	-6.1	16.5	6.9	1.1	0.5	544.6	45.3	143.5	10.0	-1.50	4.20	208
-36.7	-86.2	-5.9	15.7	7.1	1.1	0.5	509.4	49.7	133.1	9.3	-1.52	4.14	205
-40.9	-83.6	-7.0	19.5	7.8	1.7	0.7	585.1	77.7	175.3	15.5	-1.56	4.03	128
-44.8	-74.4	-6.6	19.9	8.3	2.1	0.9	494.4	48.0	199.6	21.0	-1.48	4.24	90
-48.9	-71.2	-7.8	16.0	7.2	2.1	1.0	557.0	57.9	131.6	17.6	-1.53	4.11	56
-52.4	-57.3	-5.8	14.7	6.7	2.3	1.1	330.2	42.4	92.3	14.6	-1.33	4.74	40
-56.9	-58.6	-7.0	16.3	4.6	3.8	1.1	409.3	-7.5	119.8	28.2	-1.52	4.15	18
-60.5	-44.9	-2.8	7.7	3.0	2.4	0.9	124.0	5.5	17.5	5.5	-1.29	4.88	10

Limaye and Suomi, 1981; Rossow *et al.*, 1980). Thus we know that the zonal mean circulation as determined from a relatively short duration of cloud motion observations is variable over periods as long as 5 years. While the Mariner observations were obtained from only about 8 days of imaging data, the Pioneer Venus data provides a much longer time history. In the present work images acquired on 29 days during spring and fall of 1979 were analyzed. Twenty-four of these days were between February 7, 1979, and March 29, 1979, while the remaining 5 days of imaging observations were obtained between October 15 and October 19. Although the spring

observations can be analyzed on a 4- to 5-day basis, or even a daily basis, the estimated errors in the resultant zonal mean circulation are too large to detect small variations in  $\langle u \rangle$  and  $\langle v \rangle$ . Changes over very short periods are no greater than 5 m/sec for  $\langle u \rangle$  and 2 m/sec for  $\langle v \rangle$ .

The two observing periods during 1979 present an intermediate time interval between the 5 years between Mariner 10 data and Pioneer data and the daily interval for the Pioneer data. The two sets of measurements together have approximately 6500 cloud motion vectors for the spring imaging period and over 900 for the 5 days in the fall of 1979. The results for the spring and fall

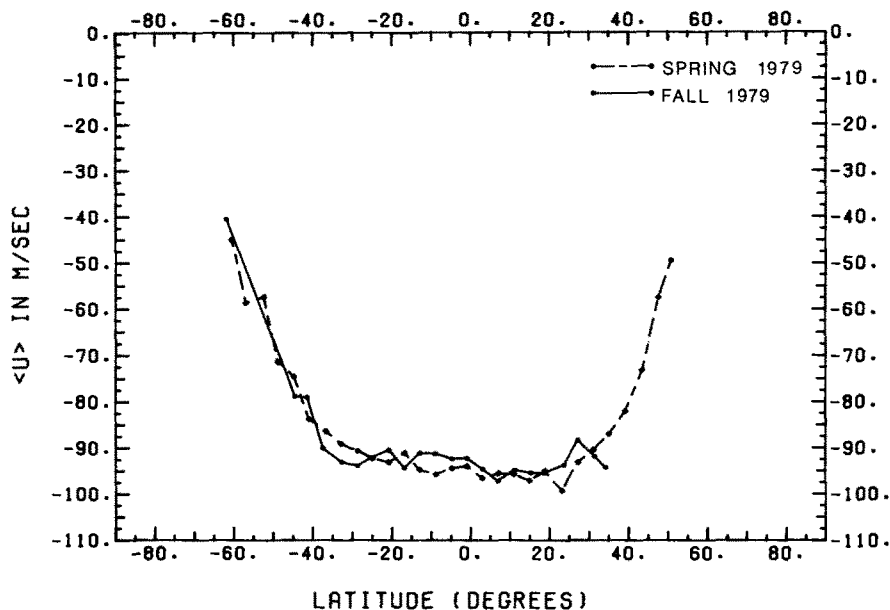
periods are presented in Tables V and VI, respectively. The latitudinal profile of  $\langle u \rangle$  for the spring and fall data is shown in Fig. 8a. Although the differences are generally smaller than 5 m/sec at most latitudes, a consistent pattern is seen. During fall 1979 the zonal mean  $u$  components are generally smaller north of about 15° south latitude, and larger south of this boundary. However, the true errors in the  $\langle u \rangle$  component are likely to be larger as mentioned before, and therefore it cannot be confidently stated that the zonal component profile with latitude changed between spring and fall of 1979. There is, however, an additional indicator of a long-term change in the mean zonal component—the rms deviation about  $\langle u \rangle$  in a given latitude bin where there are a large number of measurements available is smaller for the fall 1979 data than for the spring 1979 data. If fewer days of the spring 1979 data are analyzed so that the

number of vectors is comparable to that of the fall sample, the rms deviations are more comparable, but not sufficiently so. This may be an indication that the  $\langle u \rangle$  component varies slowly over a shorter period of only a few days, but that a long-term trend may also be present. Analysis of the observations acquired by the OCPP during the extended mission imaging opportunities which have better temporal coverage of Venus may shed some light on these trends. More cloud motion observations are required for the fall 1979 observing period to better estimate the  $\langle u \rangle$  profile.

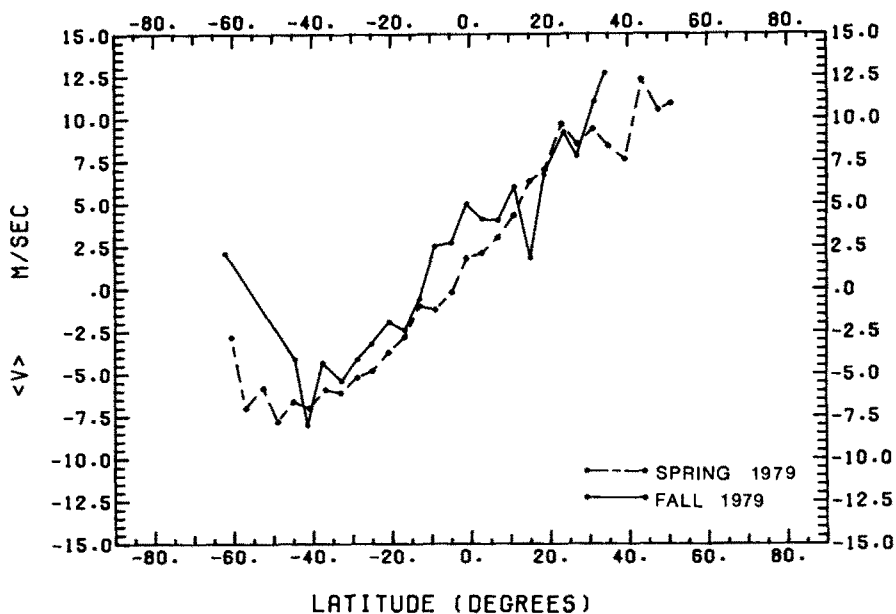
Similar systematic differences in the latitudinal profile of  $\langle v \rangle$  are also observed between the spring and fall 1979 results (Fig. 8b). The mean meridional component is generally slower at most latitudes south of 15° north latitude. Once again the differences are comparable to the likely errors involved and thus it cannot be said that the

TABLE VI  
ZONAL MEAN STATISTICS FOR FALL 1979 DATA

(Lat) (deg)	$\langle u \rangle$	$\langle v \rangle$	rms $u$	rms $v$	$E_u$	$E_v$	$\langle u \rangle \langle v \rangle$	$\langle u'v' \rangle$	rms	$E$	Omega (rad/day)	$P$ (days)	$N$
	m/sec						(m/sec) <sup>2</sup>						
34.2	-94.2	12.7	11.0	6.2	4.9	2.8	-1193.8	38.3	58.8	26.3	-1.61	3.91	5
31.3	-91.7	11.0	12.0	1.6	6.9	0.9	-1010.3	10.6	17.3	10.0	-1.52	4.15	3
27.0	-88.2	7.8	12.8	2.3	4.9	0.9	-689.9	-18.3	37.0	14.0	-1.40	4.50	7
23.6	-93.6	9.2	9.2	3.7	2.2	0.9	-859.5	-18.1	37.2	8.8	-1.44	4.35	18
18.6	-95.4	6.7	5.6	3.4	1.7	1.0	-639.5	1.0	13.2	4.0	-1.42	4.42	11
15.2	-95.3	1.8	7.4	6.7	2.3	2.1	-171.8	-13.6	37.8	12.0	-1.40	4.50	10
11.1	-94.7	6.0	7.1	4.5	1.3	0.8	-564.2	-6.7	55.1	10.1	-1.36	4.61	30
7.0	-97.1	4.0	8.1	6.5	1.3	1.0	-384.1	-13.3	50.2	7.8	-1.38	4.55	41
3.0	-94.4	4.1	5.4	7.4	0.9	1.2	-382.8	-1.0	31.2	4.9	-1.33	4.71	40
-1.0	-92.1	5.0	6.3	4.6	0.7	0.5	-462.3	5.2	27.4	3.1	-1.30	4.83	78
-4.8	-92.2	2.7	5.9	4.2	0.7	0.5	-248.7	-0.5	26.6	3.0	-1.31	4.81	79
-9.0	-91.1	2.5	6.0	4.5	0.7	0.5	-229.0	9.0	25.0	3.0	-1.30	4.83	72
-13.0	-90.9	-0.6	6.5	5.2	0.7	0.6	52.1	14.1	36.3	4.0	-1.32	4.77	82
-16.8	-94.2	-2.4	8.8	4.9	1.1	0.6	229.7	20.9	51.9	6.8	-1.39	4.52	59
-20.8	-90.3	-1.9	8.7	5.4	1.0	0.6	173.6	28.2	54.3	6.1	-1.36	4.61	80
-25.2	-92.0	-3.2	10.7	5.5	1.5	0.8	298.1	16.0	55.1	7.5	-1.44	4.38	54
-28.7	-93.8	-4.1	12.2	4.9	1.5	0.6	382.7	35.0	83.4	10.3	-1.51	4.16	65
-32.7	-92.9	-5.4	9.5	3.7	1.8	0.7	499.9	8.0	35.1	6.5	-1.56	4.03	29
-37.5	-89.9	-4.3	13.2	4.8	3.7	1.3	385.3	3.6	21.3	5.9	-1.60	3.93	13
-41.4	-78.9	-8.0	13.2	5.7	3.8	1.6	630.1	-2.0	69.3	20.0	-1.49	4.23	12
-44.5	-78.7	-4.1	20.2	4.5	6.7	1.5	320.6	75.9	113.5	37.8	-1.56	4.03	9
-61.9	-40.5	2.1	3.4	2.0	2.0	1.2	-86.5	6.8	8.4	4.8	-1.21	5.17	3



a



b

FIG. 8. Comparison of the mean meridional profiles of the (a) zonal component of motion,  $\langle u \rangle$ , for the spring and fall observations for both sets combined, and (b) for the mean meridional component of motion,  $\langle v \rangle$ , for the spring and fall data.

$\langle v \rangle$  component changed between spring and fall of 1979 either.

#### 7. SUMMARY

The most reassuring result from the present work is that measurements made by different individuals on the same set of images yield virtually the same zonal mean statistics for the cloud top circulation of Venus. Although the differences between the two sets of measurements are as large as almost 10 m/sec for  $\langle u \rangle$  and 5 m/sec for the  $\langle v \rangle$  component, the relative agreement between them is remarkable considering the long time interval between the images over which the clouds are tracked and the dynamic behavior of the Venus cloud patterns.

The mean zonal component is about  $-95$  m/sec at the equator, corresponding to a rotational period of about 4.8 days. The period of rotation increases to about 4.2 days for latitude regions  $35-45^\circ$  south and  $25-40^\circ$  north. The mean meridional motion is toward the northern pole north of  $5^\circ$  south latitude and toward the southern pole south of this latitude.

Comparison of meridional profiles of  $\langle u \rangle$  for the spring and fall 1979 periods shows some consistent differences of no more than about 5 m/sec, with the northern hemisphere speeds being higher in spring than in fall and the opposite for the southern hemisphere data, but they are smaller than the true uncertainty in the mean zonal component. These differences appear to be precursors of the even different meridional profile of  $\langle u \rangle$  that appears to be present during spring 1980 (Rossow, 1981).

Although the errors in the mean circulation momentum may amount to 20 to 30% and greater for the eddy circulation momentum transport, the mean circulation meridional momentum transport is seemingly much larger than that by the eddy circulation at the cloud top level and both are polewards, similar to the Mariner 10 results. The precise role played by the mean and eddy circulation momentum

transports in the meridional direction are as yet uncertain, considering the different circulation between Mariner 10 and Pioneer Venus observing periods. Conceivably equatorward momentum transports could exist at higher latitudes, where, unfortunately, we have no means of obtaining any estimates. Further, the vertical structure of the circulation near the cloud top levels is also unknown, although OCPP polarimetry observations may provide some clues regarding the nature of the circulation above the cloud level in the haze layers. Need for further imaging observations from the Pioneer Venus mission throughout its mission life (through 1992) is obvious from the questions about the zonal mean circulation that are yet unanswered.

Finally, information about the atmospheric circulation on the nightside of Venus would also be useful and should be considered in any future missions.

#### ACKNOWLEDGMENTS

This work was initiated and mostly completed while S.S.L. was a National Research Council Resident Research Associate at the Institute for Space Studies, NASA/Goddard Space Flight Center, New York, and support therefrom is gratefully acknowledged. Additional support was provided by a grant (NGR 50-002-189) from the National Aeronautics and Space Administration to the Space Science and Engineering Center, University of Wisconsin-Madison. Data analysis was supported by the Pioneer Venus Project Office, NASA Ames Research Center, Moffett Field, California. We thank Drs. L. Travis, W. B. Rossow, and A. D. Del Genio for many discussions during the course of this project. Thanks are also due to Lex Lane, George Wong, Nadim Habra, and many others who assisted in numerous ways. Drs. L. Sromovsky and H. Revercomb also deserve our thanks for their comments on the manuscript.

#### REFERENCES

- BELTON, M. J. S., G. R. SMITH, G. SCHUBERT, AND A. D. DEL GENIO (1976). Cloud patterns, waves and convection in the Venus atmosphere. *J. Atmos. Sci.* **33**, 1394-1417.
- COVEY, C., AND G. SCHUBERT (1981). 4-day waves in the Venus atmosphere. *Icarus* **47**, 130-138.
- DAVIES, M. E., V. K. ABALAKIN, C. A. CROSS, R. L. DUNCOMBE, H. MASURSKY, B. MORANDO, T. C.

- OWEN, P. K. SEIDELMANN, A. T. SINCLAIR, G. A. WILKINS, AND Y. S. TJUFLIN (1980). Report of the IAU working group on cartographic coordinates and rotational elements of the planets and satellites. *Celestial Mech.* **22**, 205–230.
- DEL GENIO, A. D., AND W. B. ROSSOW (1982). Temporal variability of uv features in the Venus stratosphere. *Icarus* **51**, 391–415.
- GIERASCH, P. J. (1975). Meridional circulation and the maintenance of the Venus atmospheric rotation. *J. Atmos. Sci.* **32**, 1038–1044.
- KAWABATA, K., D. L. COFFEEN, J. E. HANSEN, W. A. LANE, M. SATO, AND L. D. TRAVIS (1980). Cloud and haze properties from Pioneer Venus polarimetry. *J. Geophys. Res.* **85**, 8107–8128.
- LIMAYE, S. S. (1977). *Venus Stratospheric Circulation: A Diagnostic Study*. Ph.D. thesis submitted to the Department of Meteorology, University of Wisconsin–Madison.
- LIMAYE, S. S., AND V. E. SUOMI (1981). Cloud motions on Venus: Global structure and organization. *J. Atmos. Sci.* **38**, 1220–1235.
- ROSSOW, W. B. (1981). Paper presented at the International Conference on the Venus Environment, NASA/Ames Research Center, Palo Alto, California, November 1–6, 1981.
- ROSSOW, W. B., AND G. P. WILLIAMS (1979). Large-scale motion in the Venus stratosphere. *J. Atmos. Sci.* **36**, 377–389.
- ROSSOW, W. B., A. D. DEL GENIO, S. S. LIMAYE, L. D. TRAVIS, AND P. H. STONE (1980). Cloud morphology and motions from Pioneer Venus images. *J. Geophys. Res.* **85**, 8107–8128.
- RUSSEL, E., L. WATTS, S. PELLICORI, AND D. COFFEEN (1977). Orbiter cloud photopolarimeter for the Pioneer Venus mission. *Proc. Soc. Photo-Opt. Instrum. Eng.* **112**, 28–44.
- SCHUBERT, G., C. COVEY, A. DEL GENIO, L. S. ELSON, G. KEATING, A. SEIFF, R. E. YOUNG, J. APT, C. C. COUNSELMAN III, A. J. KLIORE, S. S. LIMAYE, H. E. REVERCOMB, L. A. SROMOVSKY, V. E. SUOMI, F. TAYLOR, R. WOO, AND U. VON ZAHN (1980). Structure and circulation of the Venus atmosphere. *J. Geophys. Res.* **85**, 8007–8025.
- SUOMI, V. E. (1974). Cloud motions on Venus. In *The Atmosphere of Venus, Proceedings of a Conference Held at the Goddard Institute for Space Studies* (J. Hansen, Ed.), NASA/GSFC, New York, 15–17 October, 1974, NASA SP-382.
- TRAVIS, L. D. (1978). Nature of the atmospheric dynamics on Venus from power spectrum analysis of Mariner 10 images. *J. Atmos. Sci.* **35**, 1584–1595.
- TRAVIS, L. D. (1979). Imaging and photopolarimetry with the Pioneer Venus Orbiter cloud photopolarimeter. *Proc. Soc. Photo-Opt. Instrum. Eng.* **183**, 299–304.
- TRAVIS, L. D., D. L. COFFEEN, J. E. HANSEN, K. KAWABATA, A. A. LACIS, W. A. LANE, S. S. LIMAYE, AND P. H. STONE (1979a). Orbiter cloud photopolarimeter investigation. *Science* **203**, 781–785.
- TRAVIS, L. D., D. L. COFFEEN, A. D. DEL GENIO, J. E. HANSEN, K. KAWABATA, A. A. LACIS, W. A. LANE, S. S. LIMAYE, W. B. ROSSOW, AND P. H. STONE (1979b). Cloud images from the Pioneer Venus Orbiter. *Science* **205**, 74–76.